ALD Al$_2$O$_3$ coatings significantly improve thermal, chemical and mechanical stability of anodic TiO$_2$ nanotube layers

Raul Zazpe[†], Jan Prikryl[†], Viera Gärtnerova[‡], Katerina Nechvilova[§], Ludvik Benes[‡], Lukas Strizik[†,‖], Ales Jäger[‡], Markus Bosund[ϕ], Hanna Sopha[†] and Jan M. Macak[†],*

[†] Center of Materials and Nanotechnologies, Faculty of Chemical Technology, University of Pardubice, nam. Cs. legii 565, 53002 Pardubice, Czech Republic.

‡ Laboratory of Nanostructures and Nanomaterials, Institute of Physics of the CAS, v.v.i., Na Slovance 2, 182 21 Prague 8, Czech Republic

[§] Institute of Chemistry and Technology of Macromolecular Materials, Faculty of Chemical Technology, University of Pardubice, Studentska 573, 532 10 Pardubice, Czech Republic

[‡] Joint laboratory of Solid-State Chemistry, Faculty of Chemical Technology, University of Pardubice, Studentska 95, 532 10 Pardubice, Czech Republic

[‖] Department of General and Inorganic Chemistry, Faculty of Chemical Technology, University of Pardubice, Studentska 573, 532 10 Pardubice, Czech Republic

[ϕ] Beneq, Olarinluoma 9, 02201 Espoo, Finland

* Corresponding Author: e-mail: jan.macak@upce.cz, Phone: +420-466 037 401

In this work, we report on a very significant enhancement of the thermal, chemical and mechanical stability of self-organized TiO_2 nanotubes layers, provided by thin Al_2O_3 coatings of different thicknesses prepared by atomic layer deposition (ALD). TiO_2 nanotube layers coated with Al_2O_3 coatings exhibit significantly improved thermal stability as illustrated by the preservation of the nanotubular structure upon annealing treatment at high temperatures (870 ^{o}C). In addition, a high anatase content is preserved in the nanotube layers, against expectation of the total rutile conversion at such a high temperature. Hardness of the resulting nanotube layers is investigated by nanoindentation measurements, and shows strongly improved values compared to uncoated counterparts. Finally, it is demonstrated that Al_2O_3 coatings guarantee unprecedented chemical stability of TiO_2 nanotube layers in harsh environments of concentrated H_3PO_4 solutions.

Introduction

Self-organized TiO$_2$ nanotube layers have attracted remarkable attention within the past 15 years due their unique architecture, high surface area, semiconductive properties and biocompatibility.[1,2] In addition, they are produced by a low-cost electrochemical anodization of Ti substrates in suitable electrolytes containing fluorides. All these features enabled utilization of TiO$_2$ nanotube layers in a wide number of applications as photocatalyst,[3,4] anode of dye-sensitized solar cells (DSSC)[5,6] and perovskite solar cells (PSC),[7,8] gas sensors[9] and biomedical materials,[10,11] among others. In all these applications, TiO$_2$ nanotube layers have shown superior performance compared to other TiO$_2$ nanostructures. In parallel, important efforts have been carried out to tune the nanotube aspect-ratio[12-14], and to improve the nanotube ordering[15-17] and crystallinity[18-20]. Annealing treatment of amorphous as-synthesized TiO$_2$ nanotube layers leads to their crystallization into anatase (> 280 ^{o}C), a combination of anatase and rutile (> 450 ^{o}C) or rutile (> 550 ^{o}C).[18-20]

The anatase nanotubular structure has shown to be more favorable than rutile for photoelectrochemically assisted applications, such as photocatalysis[3,4] and DSSC.[21,22] Thus, the stability of anatase nanotubular structure is highly desired, and numerous efforts have been focused on this target, especially at high temperatures. The introduction of alloying elements as Nb[23] or C[24] was reported to induce a shift of the anatase to rutile transition (further noted as ART) to higher temperature, and increased thermal resistance against collapse. However, the main disadvantage of alloying is the formation of undesired secondary impurity phases, e.g., Ti-Nb$_2$O$_5$.[25] The ART threshold depends on whether the nanotube layers are attached or separated from the Ti substrate. High temperature stability (up to 700 ^{o}C) of TiO$_2$ nanotube arrays, preserving the nanotubular integrity and anatase structure, was reported for free-standing TiO$_2$

nanotube arrays.[26] For TiO$_2$ nanotube layers attached to Ti substrate, anatase structure and no structural collapse was reported up to 800 $^{\circ}$C. The stability against collapse at this temperature is maintained either by a previous solvothermal treatment,[27] or previous annealing at lower temperature.[28] The highest published temperature without nanotube collapse ($\approx$ 1048 $^{\circ}$C) was reached during flame annealing process.[29] However, such flame high temperature processing led to undesired transition to rutile structure, and a significant uptake of carbon from the flame. Despite numerous efforts focused onto the high temperature stability of TiO$_2$ nanotubes layer, the temperature working window is still restricted. Another constrain for applications of TiO$_2$ nanotube layers is their limited chemical stability in harsh acidic environments, where nanotube layers undergo chemical dissolution.

The improvement of the thermal, chemical and eventually also mechanical properties of TiO$_2$ nanotube layers would enable their utilization in previously non-imaginable working environments, and surely interesting expansion of their application range. In principle, addition of a thin continuous coating of an appropriate secondary material (with excellent thermal and chemical stability) within nanotubes should significantly alter also their stabilities. So far, however, no such treatment has been shown. To date, atomic layer deposition (ALD) technique is the only method that enables homogeneous, continuous and conformal coating of secondary materials into TiO$_2$ nanotube layers. Deposition of Al$_2$O$_3$[30-33] and ZnO[34,35] coating by ALD into TiO$_2$ nanotube layers have been reported yielding interesting synergic effects. The resulting composite heterostructures revealed significant improvement of their photovoltaic and photocatalytic performance due to enhanced charge separation induced by coatings of secondary materials.

Therefore, in the present work we investigated the thermal, chemical and mechanical properties of self-organized TiO_2 nanotube layers uniformly coated with Al_2O_3 layers of different nominal thicknesses: 1, 10 and 42 nm. These coatings were carried out by atomic layer deposition (ALD) using different number of identical deposition cycles. After the Al_2O_3 coating, the TiO_2 nanotube layers were annealed at temperature up to 870 ^oC for 1 h to evaluate their thermal stability. The resulting crystal structure and composition were analyzed through X-ray diffraction (XRD), scanning transmission electron microscopy (STEM). Mechanical properties (hardness) were characterized by nanoindentation measurements using atomic force microscope. The chemical stability was tested by soaking the Al_2O_3 coated TiO_2 nanotube layers into H_3PO_4 solutions of different concentrations for 48 h at laboratory temperature and for additional 8 hours in solutions with temperature of 60°C.

Experimental Section

Self-organized TiO_2 nanotube layers with a thickness of $\approx$ 20 μm and a nanotube diameter of $\approx$ 110 nm (aspect ratio $\approx$ 180) were fabricated via anodization of Ti foils using previously published approach.[36] Prior to anodization, the Ti foils (Sigma-Aldrich 0.127 mm thick, 99.7 % purity) were degreased by sonication in isopropanol and acetone, then rinsed with isopropanol and dried in air. The electrochemical setup consisted of a 2 electrode configuration using a platinum foil as the counter electrode, while Ti foils (working electrodes) were pressed against an O-ring of the electrochemical cell, leaving 1 cm^2 open to the electrolyte. A high-voltage potentiostat (PGU-200V, IPS Elektroniklabor GmbH) was employed to carry out the electrochemical experiments at room temperature. Ethylene glycol containing 1.5 vol.% deionized water and 176 mM NH_4F was used as electrolyte. All electrolytes were prepared from

reagent grade chemicals (Sigma Aldrich). Electrolytes were aged before the first use for 15 h by anodization of blank Ti foils at 60 V under the same conditions for the anodization experiments – reasons for aging were described in the previous literature.[37] Ti foils were anodized for 4 h after sweeping the potential from 0 V to 60 V with a sweeping rate of 1 V/s. After anodization the Ti foils were rinsed and sonicated in isopropanol and dried.

The TiO_2 nanotube layers by were coated with Al_2O_3 by atomic layer deposition tool (thermal ALD, TFS 200, Beneq). This technique based on sequential and self-limiting gas-surface reactions, allows conformal deposition of various coatings within TiO_2 nanotube layers with a nanometer scale accurate thickness, as shown previously.[36,38] Trimethylaluminum (TMA, Strem, elec. grade, 99.999+ %) and deionized water (18 MΩ) were used as aluminum and oxygen precursors, respectively. Under these deposition conditions, one growth ALD cycle was defined by the following sequence: TMA pulse (1 s)-N_2 purge (3 s)-H_2O pulse (1 s)-N_2 purge (3 s). All processes were carried out at a temperature of 200 ^oC, and using N_2 (99.9999 %) as carrier gas at a flow rate of 400 standard cubic centimeters per minute (sccm). Al_2O_3 deposition was carried out running 8, 88 and 366 ALD cycles, leading to coatings of different nominal thicknesses: 1, 10 and 42 nm, respectively. The number of cycles required for the different Al_2O_3 thicknesses was estimated from the growth per cycle value of the Al_2O_3 process at 200 ^oC (≈ 1.1 Å /cycle). The thicknesses of Al_2O_3 coating were confirmed by variable angle spectroscopic ellipsometry (VASE® ellipsometer, J.A. Woollam, Co., Inc.) of Al_2O_3 coatings on Si wafers.

Upon the Al_2O_3 coating process, the TiO_2 nanotube layers were annealed along with reference uncoated layers. The annealing process was carried out in a muffle oven in an air atmosphere applying a heating rate of 15 ^oC/min, until the target temperature (870 ^oC) was

reached. The annealing process proceeded at such temperature for 1 h. Afterwards the layers were allowed to naturally cool down.

The morphology of the TiO_2 nanotube layers was characterized by a field-emission SEM (FE-SEM JEOL JSM 7500F) and a scanning transmission electron microscope (STEM, FEI Tecnai F20 X-Twin) fitted with a high angle annular dark field (HAADF) detector and operating at 200 kV. The cross-sectional views were obtained from mechanically bent samples. Due to the rupture of the nanotube layers via this bending, it was possible to visualize nanotubes within the layers and coatings within nanotubes in various directions and nanotube layer depths. Dimensions of the nanotubes were measured and statistically evaluated using proprietary Nanomeasure software. Average values and standard deviations were calculated from at least 3 different locations with a high number of measurements (n > 100).

Diffraction analyses of the Al_2O_3 coated TiO_2 nanotube layers carried out using X-ray diffractometer (XRD, D8 Advance, Bruker AXE) using Cu *Ka* radiation with secondary graphite monochromator and Na(Tl)I scintilation detector.

Nanoindentation measurements were performed to analyze the mechanical properties (hardness) of the TiO_2 nanotube layers. They were determined by atomic force microscope (AFM, SOLVER NEXT, NT MDT) equipped with a nanoindentation head NS01NTF, and a Berkovich type of tip (three-sided pyramid geometry with a parameter of static stiffness, k = 10.2 ± 0.3 kN/m). The nanotube layers were measured in longitudinal direction for compressive force of 0.5 mN, loaded for 100 s. Fused silica SiO_2 was used as a calibration sample (hardness, H = 9.5 ± 0.5 GPa by ISO 9450-76). The penetration depth of the tip was up to a maximum 10 % of the total thickness of the nanotube layer The hardness was evaluated at ~30 different areas of each nanotube layer to ensure statistically relevant data set/significant results.

The chemical stability of Al_2O_3 coated TiO_2 nanotube layers was analyzed by soaking in H_3PO_4 solutions of different concentrations: 25, 50, 70 and 85 wt. % (prepared from 85 wt. % H_3PO_4, Penta). TiO_2 nanotube layers were soaked in these solutions for 48 h, including a thermal treatment for 8 h by which solutions were heated up at 60 ^{o}C to further study the nanotube chemical stability under warm acidic conditions. Before the subsequent SEM analysis, the layers were rinsed with water and dried in air.

Results and Discussion

Al_2O_3 COATING OF TiO_2 NANOTUBE LAYERS

Highly ordered TiO_2 nanotube layers, with a thickness of $\approx$ 20 μm and an average diameter value of $\approx$ 110 nm (aspect ratio $\approx$ 180), were prepared by anodization of Ti foils as described in detail in the experimental section. As-prepared amorphous TiO_2 nanotube layers were coated with Al_2O_3 of different nominal thicknesses, namely 1, 10 and 42 nm by ALD, as verified by SEM and ellipsometric measurements (1.1 ± 0.2, 10 ± 0.5, and 44 ± 2.1 nm). Freshly coated nanotube layers were annealed at 870 ^{o}C for 1 h along with reference uncoated TiO_2 nanotube layers. Figure 1 shows SEM images of the TiO_2 nanotube layers with and without Al_2O_3 coating annealed at 870 °C. Uncoated TiO_2 nanotube layers (Figure 1a) collapsed during the annealing process into a pillar nanostructure (Figure 1b). When coated, the nanotube layers were preserved after the annealing process, regardless the thickness of the Al_2O_3, as apparent for coating of either 1 nm (Figure 1c-d), or 10 nm (Figure 1e-f). It is quite fascinating that even 1 nm thin Al_2O_3 coating can built a very thermally robust cage all over TiO_2 nanotubes with some 20-40 nm thick tube walls.

Figure 2 shows representative STEM-HAADF images of the nanotube body (separated from the annealed Al_2O_3 coated (10 nm) TiO_2 nanotube layer by mechanical bending of the layers followed by sonication in methanol) at a low (a) and at a high magnification (b). Especially from Figure 2b, the interface between the TiO_2 wall and Al_2O_3 coating is well distinguishable. There are actually two interfaces between the TiO_2 wall and Al_2O_3 coating, as the Al_2O_3 coating is deposited inside (interior coating) and outside (exterior coating) the TiO_2 tube walls. This feature is in accordance with our previous ALD work[36], where we showed very good uniformity of Al_2O_3 coatings on the amorphous tubes and absence of any pinholes in the coating. As apparent from Figure 2, Al_2O_3 coatings remained continuous and pinhole-free even after annealing, during which thermally induced crystallization of TiO_2 tube walls occurred. Some delamination of the coating seen at the outer and inner interface between TiO_2 wall and Al_2O_3 coating (especially at Fig. 2b) stems most likely from the stress that these layers are exposed to during the preparation of specimens for SEM and STEM observation, which includes mechanical rupture of layers. These roughening and delamination events have no detrimental effect on coated nanotube layers that were not submitted for SEM and STEM and that completely survived soaking in H_3PO_4 solutions (described later in text).

INFLUENCE OF THE COATING ON CRYSTAL STRUCTURE

It is generally accepted that the annealing process influences crystal structure, phase transition and structural integrity of the TiO_2 nanotube layers.[18-20] It has also been accepted that amorphous as-prepared TiO_2 nanotube layers crystallize into anatase above 280 °C in air.[2] The anatase to rutile transition (ART) has been reported at different temperatures, most usually in the range of temperature between 500 and 600 °C, depending on the nanotube dimensions (diameter,

thickness, composition). Annealing at temperatures higher $\geq 600\ ^{o}C$ leads to the coexistence of anatase and rutile structures, while total conversion to rutile structure takes place above $800\ ^{o}C$.[2,39]

Figure 3a shows the XRD pattern obtained for reference uncoated TiO_2 nanotube layers annealed for 1 h at either 400 or 870 ^{o}C, respectively. In line with literature, the former exhibits pure anatase crystal phase identified by typical anatase peaks associated with planes (101), (004), (105), and (211), with a dominant orientation (101). The latter reveals pure rutile crystal phase with well-defined diffraction peaks of planes (110), (011), (111), (211), and (220). The intensity of the peak at $2\theta = 27.4^{o}$ indicates a preferred orientation along the (110) direction; no trace of anatase polymorphic phase is detected.

The XRD patterns, obtained from Al_2O_3 coated TiO_2 nanotube layers annealed at 870 ^{o}C for 1 h, are shown in Figure 3b. Therein the coexistence of anatase and rutile structures can be clearly seen, in contrast to the uncoated nanotube layers (Figure 3a) where rutile was exclusively formed at this temperature, in line with the previous work.[18] The incomplete ART of coated TiO_2 nanotube layers annealed at 870 ^{o}C stems from the hindered surface reconstruction of the TiO_2 due to Al_2O_3 coating and also the impact of Al^{3+} as the phase transformation inhibitor.[40] In contrast, for uncoated nanotube layers (annealed at 870 ^{o}C) the surfaces reconstruction can easily take place (no space constrains are present), allowing for the mass flow and rearrangements that yield complete rutile conversion, expected at this temperature.[18] Another evidence for limited reconstruction of coated TiO_2 nanotube layers annealed at 870 ^{o}C is the fact, that they do not collapse (sinter), which they would otherwise do without coating. In the case of thermally stable coated nanotube layers, the coating acts in similar fashion as it does for nanoparticles and nanorods that can be annealed, when coated, at high temperatures without undergoing sintering

events.[41,42] Quantification of the content of each crystal phase and an average of the corresponding crystallite size are given in Table 1.

The anatase : rutile ratio was found to be dependent on the Al_2O_3 coating. The nanotube layer with the thickest Al_2O_3 coating (42 nm) exhibited dominant rutile structure (62%) with peaks corresponding to the planes (110) (001) (111) (211) and (220), and only one minor anatase peak corresponding to (101) plane. In clear contrast, the anatase content for 10 nm and 1 nm thin Al_2O_3 coating was found to increase up to 73 % and 83 %, respectively, on account of rutile. In addition, identical rutile peaks were revealed for them as for the nanotube layer with thickest Al_2O_3 coating (42 nm). It is noteworthy that the 1 nm thin Al_2O_3 coated nanotube layer revealed anatase peaks with preferential orientation along the (004) plane, instead of usual (101) plane. This feature was already reported by Acevedo et al.,[39] who associated a particular thermal stability of the nanotube layers to such anatase (004) plane. Based on the XRD results in Figure 3b, there is obvious retardation of the anatase to rutile transition (further noted as ART) with decreasing thickness of Al_2O_3 coatings (1 and 10 nm).

In order to give a physical description of the results, factors affecting the ART need to be discussed. Firstly, we should consider the influence of the number of oxygen vacancies within the TiO_2 on the ART temperature. Rath et al.[43] reported that the larger is the number of oxygen vacancies within TiO_2, the lower is its ART temperature, or the ART does not proceed at all and TiO_2 remains in anatase form. The defects (in this case oxygen vacancies) provide a low energy mass transport route and lower such ART temperature.[44] The number of oxygen vacancies within TiO_2 is also strongly influenced by the annealing atmosphere. Previous works clearly indicated that dry annealing atmospheres such as Ar[18] or CO,[45] led to more oxygen vacancies in TiO_2 than

those performed in O_2 or air. Thus, the ART was enhanced in oxygen-free atmospheres and resulted into larger rutile crystallites.[18]

Secondly it is important to define the fundamental reasoning behind the ART origin, which has been subject of controversy. Varghese et al.[46] located the ART to proceed on the Ti substrate-TiO_2 nanotube interface, where Ti metal would be directly thermally oxidized into rutile structure. The presence of oxygen vacancies in between the Ti substrate and TiO_2 nanotube layer, was believed to induce the ART at such interface, spreading towards the whole nanotube walls in the course of time, as reported by Zhu et al.[47] In contrast, Yu et al.[48] proposed that ART does not stem from metal Ti, but from the anatase (created at lower temperatures, while ramping up the temperature) at the interface between TiO_2 nanotubes and Ti substrate, which converts to rutile at temperatures $\geq$ 600 ^{o}C. In addition, works on annealing and crystallization of free-standing nanotube layers[11,49] (i.e. nanotubes were detached from the Ti substrate before annealing) reported both the preservation of the anatase structure in the nanotube walls at temperatures higher than 600 ^{o}C, and much higher triggering ART temperature. Those results would point on a significant role of metal Ti substrate-TiO_2 nanotube interface on the ART.

There is a clear link between the experimental results obtained in this work, and the literature about factors affecting the ART.[43,44] According to Figure 3, the anatase : rutile ratio is clearly dependent on the Al_2O_3 coating thickness. Assuming the results by Rath et al.[43] that larger number of oxygen vacancies promotes the ART, it is clear that the Al_2O_3 coating within our TiO_2 nanotube layers influences the number of oxygen vacancies as it possesses a barrier against the oxygen diffusion.[50] For example, the thickest Al_2O_3 coating (42 nm) hinders the oxygen diffusion most significantly from all used coatings in this work, leads to highest number of oxygen vacancies within TiO_2 nanotubes, and boosts the ART process that ends up with the

highest rutile content. In contrast, the oxygen diffusion into TiO_2 takes place more easily through thinner Al_2O_3 coatings (1 and 10 nm), resulting in a lower number of oxygen vacancies, retarding the ART within TiO_2 nanotubes. In addition, the largest rutile crystal size, calculated by Scherrer equation (Table 1), corresponds to the thickest Al_2O_3 coating, which also corroborates previously published findings on ART and size of rutile crystals.[45,46]

To get a complete picture about the ART, we also fully explored anatase TiO_2 nanotube layers (annealed at 400 ^{o}C for 1 h), shown in Figure 3a, for Al_2O_3 coating. We coated these nanotube layers with 1 and 10 nm of Al_2O_3 by ALD, before undergoing a second thermal treatment at 870 ^{o}C for 1h. Firstly, the Figure 3c shows that the Al_2O_3 coated (10 nm) TiO_2 nanotube layer consisted of 100 % rutile, while in the Al_2O_3 coated (1nm) TiO_2 nanotube layer rutile content was only 26 %. These results confirm the active role of the Al_2O_3 coating for TiO_2 crystal structure and are in line with the results and theories discussed in Figure 3b. Secondly, the significantly different crystal structure of the both investigated types of Al_2O_3 (10 nm) TiO_2 nanotube layer were revealed. The formerly annealed Al_2O_3 coated (10 nm) TiO_2 nanotube layer (fully anatase comprised), underwent a complete ART and was 100 % rutile comprised (see Figure 3c). In contrast, the initially amorphous TiO_2 nanotube layer revealed a predominant anatase content of $\approx$ 74% (see Figure 3b). This comparison clearly confirms that the TiO_2 structure influences the ART, and that it is clearly promoted for the TiO_2 nanotube layers annealed to anatase before ART and ALD coating. In other words, the lack of coating induces during the thermal annealing to 400°C more oxygen vacancies in the TiO_2 nanotube layers than it does when coatings are present during this annealing step.

MECHANICAL PROPERTIES

The mechanical integrity of the TiO_2 nanotube layers is of significant importance, especially for synthesis of devices based on flow-through membranes utilizing nanotube layers opened on both sides.[51] Even though some nanoindentation analyses of the TiO_2 nanotube arrays were already carried out,[52-59] nanotube layers modified with additional coatings, as in the present case, have not yet been analysed. Figure 4 shows hardness of TiO_2 nanotube layers with Al_2O_3 coatings of different thicknesses as well as two reference nanotube layers. If not denoted otherwise, all nanotube layers were annealed at 870 °C for 1h as the last processing step. The obtained hardness values show two prominent features. First, the uncoated amorphous (i.e., did not undergo annealing) TiO_2 nanotube layer displayed lower hardness value than the annealed uncoated counterpart, fully rutile structure comprised. That was expected as the crystal structure has (as a rule of thumb) higher hardness than amorphous mass of the same compound. Second, the annealed Al_2O_3 coated TiO_2 nanotube layers exhibited larger hardness with the increasing Al_2O_3 coating thickness. This can be ascribed to increasing content of rutile (Table 1) and to an increasing Al_2O_3 mass within the nanotubes.

Even tough rutile and anatase are similar in structure, the reason to rutile to be more mechanically robust than anatase is that its octahedra shares four edges instead four corners (anatase case) which leads to the formation of chains arranged subsequently in a four-fold arrange.[57,59] This also explains why the Al_2O_3 coated (1 nm) TiO_2 coated layer (which has mainly anatase structure as shown in Figure 3b) has lower hardness than uncoated annealed layers (completely rutile based, also shown in Figure 3a).

The hardness values presented here for high aspect ratio (≈ 180) nanotube layers were larger than those found in literature, that reports typical hardness in the range from 94 MPa to

≈ 3.5 GPa.[52,54,57,58] However, it is difficult to establish a comparison, principally because the published reports show results for exclusively uncoated and lower aspect ratio TiO_2 nanotubes layers with thicknesses from ≈ 625 nm to 8.5 μm (compared to 20 μm in the present case). Moreover, the use of different indenter tips (Vickers tips for microhardness, Berkovitch tips for nanohardness, cube corner tips for nanohardness, etc.) entails different hardness values. Nevertheless, it can be concluded that both the annealing treatment and the Al_2O_3 ALD coating resulted in a substantial enhancement of the mechanical properties of TiO_2 nanotube layer.

CHEMICAL STABILITY

Finally, the chemical stability of Al_2O_3 coated TiO_2 nanotube layers was investigated in strongly acidic environment, namely in H_3PO_4 solutions with different concentration. Such stability is significant for the nanotube layers to sustain in environments, where up to now they could not preserve their morphological integrity. For example in various biological environments with low pH, the knowledge about the stability threshold is important. As it can be seen in Figure 5, even the thinnest coating (1 nm Al_2O_3) completely preserved the TiO_2 nanotube layers from degradation in concentrated H_3PO_4. In line with that, no degradation was observed for any of the thicker Al_2O_3 coatings - 10 and 42 nm (data not shown here). The soaking tests were performed on the 40 h time scale for all nanotube layers. The Al_2O_3 coated ones survived without any change in H_3PO_4 of all used concentrations. This expands the already wide range of environments, where ALD Al_2O_3 coatings are stable, in addition to published stability results of these coatings in various acidic (H_2SO_4, HNO_3, HCl) and alkaline (KOH) environments,[60] and water.[61] To make the H_3PO_4 environment even more harsh, the H_3PO_4 solutions were heated up to 60°C and soaking was carried out for additional 8 h (in total 48 h). Since again no visible

changes were observed, soaking experiments were terminated afterwards. Reference uncoated layers (namely as-anodized amorphous and annealed (400°C for 1h) nanotube layers) did not survive these conditions. In order to determine the chemical threshold conditions for these reference uncoated layers, lower H_3PO_4 concentrations had to be used. The stability threshold was revealed to be 10 wt. % (Figure 5e) and 24 wt. % (Figure 5f) on the scale of 24 hours for the amorphous and annealed case, respectively, without any heating. All in all, the results presented in Figure 5 for Al_2O_3 coated nanotube layers confirm the outstanding enhancement of the chemical stability of TiO_2 nanotube layers provided by uniform Al_2O_3 coatings.

Thus, the present results, especially for the thinnest Al_2O_3 coating (1 nm), are very useful and promising for practical applications of the nanotube layers. As-treated TiO_2 nanotube layers: i) maintain anatase structure (more favorable for photovoltaics and photocatalysis than rutile) in the tubes over a very broad temperature range, ii) possess significantly improved charge separation on the interface with various electrolytes (especially because electrons can tunnel to TiO_2 via Al_2O_3 coatings thinner than ≈ 2 nm[62]), iii) possess strong mechanical integrity, and iv) provide extremely good stability in strongly acidic environments. All these features pave favorable way for the functionalization of TiO_2 nanotube layers by secondary materials. It is foreseen that additional materials, such us various oxides, nitrides, sulfides, etc. may further expand the range of applications of TiO_2 nanotube layers. Thermal and chemical stability of Al_2O_3 coated TiO_2 nanotube layers can extend the utilization of nanotube layers for catalytic applications and sensing of gases (such as CO, NO_x, CH_3CH_2OH, H_2, and O_2) at high temperatures and/or in harsh acidic environment, so far unfeasible for uncoated TiO_2 nanotube layers counterparts. In parallel, membranes composed of ultrahigh aspect ratio TiO_2 nanotube layers that have been used for photocatalytic or flow-through experiments,[51] may be prone to

mechanical instabilities. Thus, they could greatly benefit from a thin Al_2O_3 coating to become mechanically more robust.

Conclusions

In this work, effects of Al_2O_3 coating produced by ALD on the crystal structure, mechanical and chemical properties of TiO_2 nanotube layers were explored. Noteworthy improvement of the thermal stability upon annealing in air was revealed up to temperatures of 870 ^{o}C, even with an extremely thin Al_2O_3 coating (1 nm). In contrast to uncoated TiO_2 nanotube layers (100 vol. % rutile), a high fraction of anatase structure (83 vol. %) was determined for Al_2O_3 coated (1 nm) TiO_2 nanotube layers upon annealing at 870 °C, which is highly desired due to its optical and electronic properties for photovoltaic and photocatalytic applications. An enhanced hardness was revealed for Al_2O_3 coated TiO_2 nanotube layers with a positive impact on the mechanical properties of nanotube layers. In addition, Al_2O_3 coatings provided to the TiO_2 nanotube layers extremely good stability in extremely acidic environments of H_3PO_4 solutions with different concentrations. All in all, self-organized TiO_2 nanotube layers coated with thin Al_2O_3 coatings yield superior thermal, chemical and mechanical stabilities that will extend their application range to previously non-imaginable working environments.
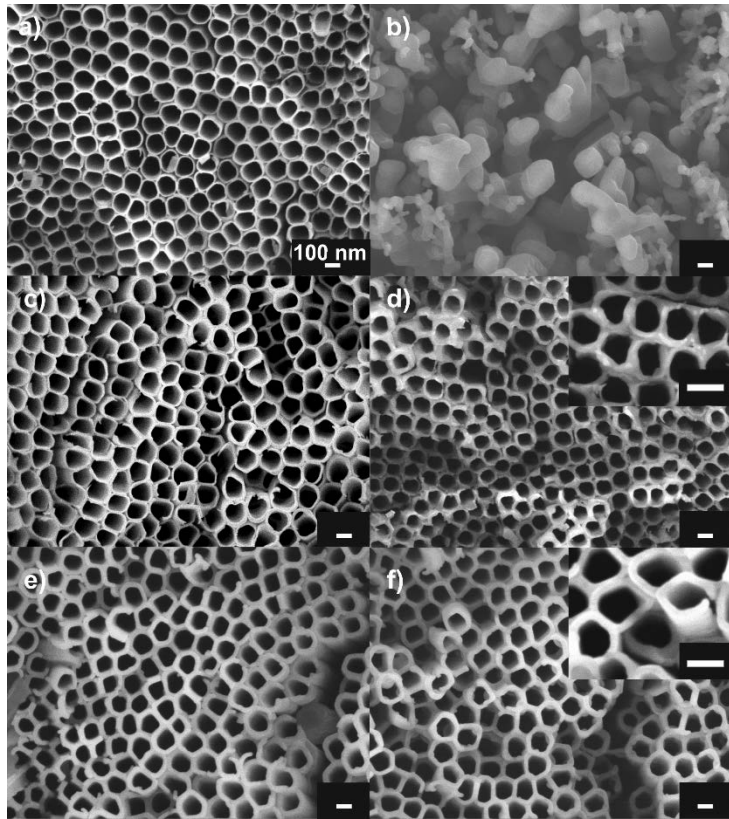
FIGURES

Figure 1. SEM top-view images of uncoated TiO_2 nanotube layer (a) before and (b) after annealing; Al_2O_3 coated (1 nm) TiO_2 nanotube layer (c) before and (d) after annealing; Al_2O_3 coated (10 nm) TiO_2 nanotube layer (e) before and (f) after annealing. The annealing was carried out at 870 ^{o}C for 1 h. Insets: magnification of the corresponding SEM images. All the scale bars denote 100 nm.
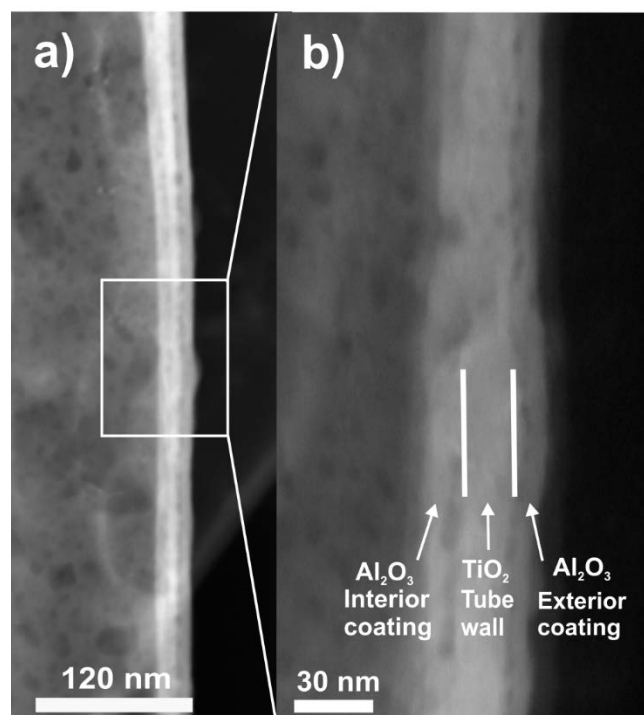
Figure 2. Representative STEM-HAADF images of (a) a fragment of Al_2O_3 coated (10 nm) TiO_2 nanotube, and (b) the corresponding higher magnification of the nanotube wall. Interfaces between individual parts of the tubes are distinguished by solid lines, and appropriate description.
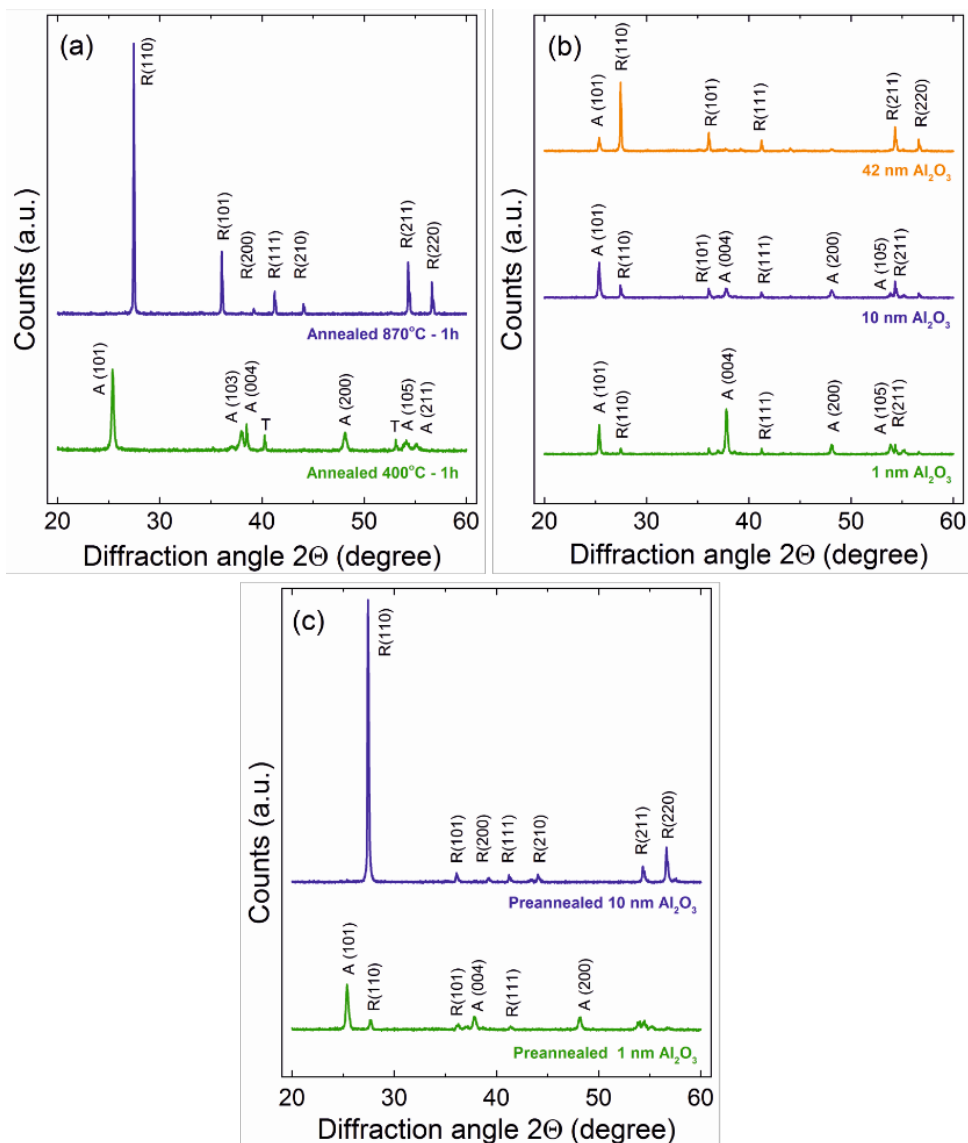
Figure 3. XRD patterns of a) uncoated TiO_2 nanotube layers annealed at 870 °C and 400 °C for 1 h; b) Al_2O_3 coated TiO_2 nanotube layers with different coating thicknesses (1, 10 and 42 nm) annealed at 870 °C for 1 h; c) Al_2O_3 coated (1 and 10 nm) TiO_2 nanotube layers pre-annealed (400 °C, 1 h) and second annealing at 870 °C. A = anatase, R = rutile, T = titanium substrate.
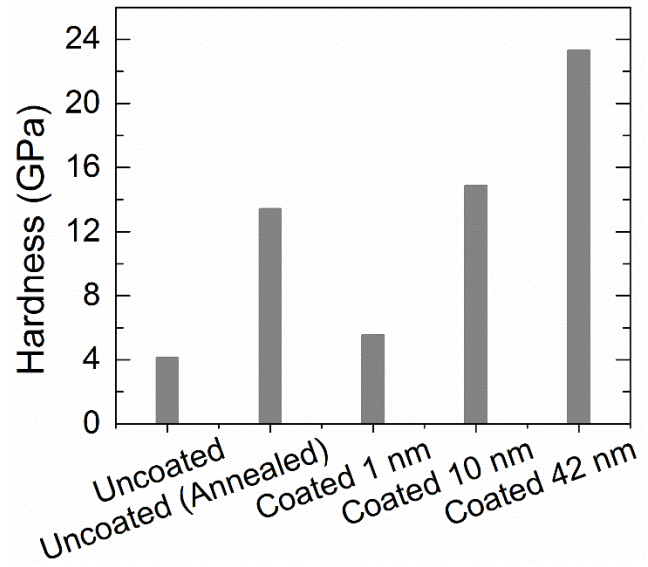
Figure 4. Hardness of different TiO$_2$ nanotube layers determined by nanoindentation measurements. Except the sample marked "uncoated", all nanotube layers were annealed at 870 °C for 1 h.
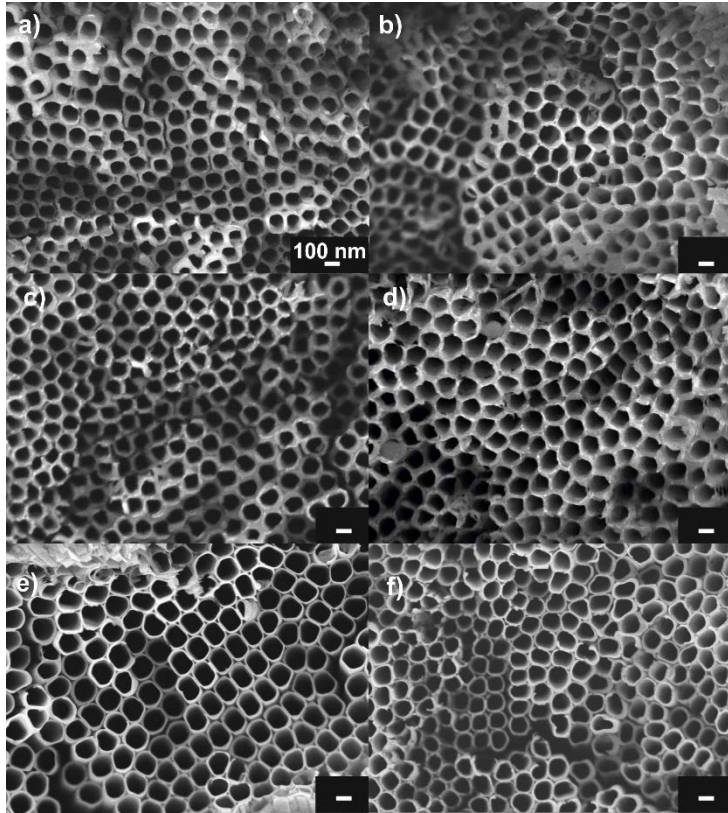
Figure 5. SEM top-view images of annealed Al_2O_3 coated (1nm) TiO_2 nanotube layers before (a) and after soaking in H_3PO_4 solutions with different concentration: (b) 50 wt. %, (c) 70 wt. % and (d) 85 wt. % in total for 48 h (last 8 h at 60 ^{o}C). SEM top-view images of reference uncoated amorphous (e) and anatase (f) TiO_2 nanotube layers after soaking in H_3PO_4 solutions of 10 and 40 wt. %, respectively, for 24 h. All the scale bars denote 100 nm.

TABLES

Table 1. Percentage of anatase and rutile TiO_2 crystal phase and the corresponding crystallite size, determined for the annealed and pre-annealed (400 ^{o}C, 1 h) TiO_2 nanotube layers with different Al_2O_3 coating thicknesses after annealing at 870 ^{o}C for 1 h.

Al_2O_3 coating thickness (nm)	Anatase (vol.%)	Crystallite Size (nm)	Rutile (vol.%)	Crystallite Size (nm)
0	0	-	100	112.9
1	83	78.4	17	93.5
10	73	52.3	27	81.5
42	38	54.4	62	129.5
Pre-annealed 1	74	29.8	26	39.4
Pre-annealed 10	0	-	100	70.5

AUTHOR INFORMATION

Corresponding Author

Jan M. Macak, E-mail: jan.macak@upce.cz

REFERENCES

(1) Macak, J. M.; Tsuchiya, H.; Ghicov, A.; Yasuda, K.; Hahn, R.; Bauer, S.; Schmuki, P. TiO_2 nanotubes: Self-Organized Electrochemical Formation, Properties and Applications. *Curr. Opin. Solid State Mater. Sci*. **2007**, *11*, 3-18.

(2) Lee, K.; Mazare, A.; Schmuki, P. One-Dimensional Titanium Dioxide Nanomaterials: Nanotubes. *Chem. Rev.* **2014**, *114*, 9385-9454.

(3) Macak, J. M.; Zlamal, M.; Krysa, J.; Schmuki, P. Self-Organized TiO_2 Nanotube Layers as Highly Efficient Photocatalysts, *Small* **2007**, *3,* 300-304.

(4) Liu, N.; Paramasivam, I.; Yang, M.; Schmuki, P. Some Critical Factors for Photocatalysis on Self-Organized TiO_2 Nanotubes. *J. Solid State Electrochem.* **2012**, *16*, 3499-3504.

(5) Macak, J. M.; Tsuchiya, H.; Ghicov, A.; Schmuki, P. Dye-sensitized Anodic TiO_2 Nanotubes. *Electrochem. Commun.* **2005**, 7, 1133-1137.

(6) Mohammapour, F., Moradi, M.; Cha, G.; So, S.; Lee, K.; Altomare, M.; Schmuki, P. Comparison of Anodic TiO_2-Nanotube Membranes used for Frontside-Illuminated Dye-Sensitized Solar Cells. *ChemElectroChem.* **2015**, *2*, 204-207.

(7) Gao, X.; Li, J.; Baker, J.; Hou, Y.; Guan, D.; Chen, J.; Yuan, C. Enhanced Photovoltaic Performance of Perovskite $CH_3NH_3PbI_3$ Solar Cells with Freestanding TiO_2 Nanotube Array Films. *Chem. Commun.* **2014**, *50*, 6368-6371.

(8) Salazar, R.; Altomare, M.; Lee, K.; Tripathy, J.; Kirchgeorg, R.; Nguyen, N. T.; Mokhtar, M.; Alshehri, A.; Al-Thabati, S. A.; Schmuki, P. Use of Anodic TiO_2 Nanotube Layers as

Mesoporous Scaffolds for Fabricating $CH_3NH_3PbI_3$ Perovskite-based Solid-State Solar Cells. *ChemElectroChem.* **2015**, *2*, 824-828.

(9) Varghese, O. K.; Gong, D.; Paulose, M.; Ong, K. G.; Grimes, C. A. Hydrogen Sensing Using Titania Nanotubes. *Sens. Actuators B* **2003**, *93*, 338-344.

(10) Gulati, K.; Ramakrishnan, S.; Aw, M. S.; Atkins, G. J.; Findlay, D.M.; Losic, D. Biocompatible Polymer Coating of Titania Nanotube Arrays for Improved Drug Elution and Osteoblast Adhesion. *Acta Biomater.* **2012**, *8*, 449-456.

(11) Kulkarni, M,; Mazare, A,; Gongadze, E.; Perutkova, S,; Kralj-Iglic, V.; Milosev, I,; Schmuki, P.; Iglic, A.; Mozetic, M. Titanium Nanostructures for Biomedical Applications. *Nanotechnology* **2014**, *26*, 062002.

(12) Macak, J. M.; Tsuchiya, H.; Schmuki, P. High-Aspect-Ratio TiO_2 Nanotubes by Anodization of Titanium. *Angew. Chem. Int. Ed.* **2005**, *44,* 2100-2102.

(13) Macak, J. M.; Tsuchiya, H.; Taveira, L.; Aldabergerova, S.; Schmuki, P. Smooth Anodic TiO_2 Nanotubes. *Angew. Chem. Int. Ed*. **2005**, *44*, 7463-7465.

(14) Albu, S. P.; Ghicov, A.; Macak, J. M.; Schmuki, P. 250 µm Long Anodic TiO_2 Nanotubes with Hexagonal Self-Ordering. *Phys. Stat. Sol. (RRL)* **2007**, *1*, R65-R67.

(15) Macak, J. M.; Albu, S.; Schmuki, P. Towards Ideal Hexagonal Self-Ordering of TiO_2 Nanotubes. *Phys. Stat. Sol. (RRL)* **2007**, *1*, 181-183.

(16) Wang, D.; Yu, B.; Wang, C.; Zhou, F.; Liu, W. A Novel Protocol Toward Perfect Alignment of Anodized TiO_2 Nanotubes. *Adv. Mater*. **2009**, *21,* 1964-1967.

(17) Sopha, H.; Jäger, A.; Knotek, P.; Tesar, K.; Jarosova, M.; Macak, J. M. Self-Organized Anodic TiO_2 Nanotube Layers: Influence of the Ti substrate on Nanotube Growth and Dimensions. *Electrochim. Acta*, **2016**, *190*, 744-752.

(18) Ghicov, A.; Tsuchiya, H.; Macak, J. M.; Schmuki, P. Annealing Effects on the Photoresponse of TiO_2 Nanotubes. *Phys. Stat. Sol. (RRL)* **2006**, *203*, R28-R30.

(19) Albu, S. P.; Ghicov, A.; Aldabergenova, S.; Drechsel, P.; LeClere, D.; Thomson, G. E.; Macak, J. M.; Schmuki, P. Formation of Double-Walled TiO_2 Nanotubes and Robust Anatase Membranes. *Adv. Mater.* **2008**, *20*, 4135-4139.

(20) Macak, J. M.; Aldabergerova, S.; Ghicov, A.; Schmuki, P. Smooth Anodic TiO_2 Nanotubes: Annealing and Structure. *Phys. Status Solidi A* **2006**, *203*, R67-R69.

(21) Mohammadpour, F.; Moradi, M.; Lee, K.; Gha, G.; So, S.; Kahnt, A.; Guldi, D.M.; Altomare, M.; Schmuki, P. Enhanced Performance of Dye-Sensitized Solar Cells on TiO_2 Nanotube Membranes Using an Optimized Annealing Profile. *Chem. Commun.* **2015**, *51*, 1631-1634.

(22) Mirabolghasemi, H.; Liu, N.; Lee, K.; Schmuki, P. Formation of 'Single Walled' TiO_2 Nanotubes with Significantly Enhanced Electronic Properties for Higher Efficiency Dye Sensitized Solar Cells. *Chem. Commun.* **2013**, *49*, 2067-2069.

(23) Arbiol, J.; Cerda, J.; Dezanneau, G.; Cicera, A.; Peiro, F.; Cornet, A.; Morante, J. R. Effects of Nb Doping on the TiO_2 Anatase-to-Rutile Phase Transition. *J Appl Phys*. **2002**, *92*, 853-861.

(24) Tryba, B.; Moravski, A. W.; Inagaki, M. A New Route for Preparation of TiO_2-Mounted Activated Carbon. *Appl Catal B: Environ*. **2003**, *46*, 203-208.

(25) Ghicov, A.; Aldabergerova, S.; Tsuchiya, H.; Schmuki, P. TiO_2–Nb_2O_5 Nanotubes with Electrochemically Tunable Morphologies. *Angew Chem Int Ed*. **2006**, *45*, 6993-6996.

(26) Lin, J.; Guo, M.; Yip, C. T.; Lu, W.; Zhang, G.; Liu, X.; Zhou, L.; Chen, X.; Huang. H. High Temperature Crystallization of Free-Standing Anatase TiO_2 Nanotube Membranes for High Efficiency Dye-Sensitized Solar Cells. *Adv. Funct. Mater*. **2013**, *23*, 5952-5960.

(27) Rao, B. M.; Roy, S. C. Anatase TiO_2 Nanotube Arrays with High Temperature Stability. *RSC Adv*. **2014**, *4*, 38133-38139.

(28) Mohammadpour, F.; Altomare, M.; So, S.; Lee, K.; Mokhtar, M.; Alshehri, A.; Al-Thabaiti, S. A.; Schmuki, P. High-Temperature Annealing of TiO_2 Nanotube Membranes for Efficient Dye-Sentitized Solar Cells. *Semicond. Sci. Technol*. **2016**, *31*, 014010 (8pp).

(29) Mazare, A.; Paramasivam, I.; Schmidt-Stein, F.; Lee, K.; Demetrescu, I.; Schmuki, P. Flame Annealing Effects on Self-Organized TiO_2 Nanotubes. *Electrochim. Acta* **2012**, *66*, 12-21.

(30) Gao, X.; Guan, D.; Huo, J.; Chen, J.; Yuan, C. Free Standing TiO_2 Nanotube Array Electrodes with an Ultra-Thin Al_2O_3 Barrier Layer and $TiCl_4$ Surface Modification for Highly Efficient Dye Sensitized Solar Cells. *Nanoscale* **2013**, *5 (21)*, 10438-10446.

(31) Jae-Yup, K.; Kyeong-Hwan, L.; Junyoung, S.; Sun Ha, P.; Jin Soo, K.; Kyu Seok, H.; Myung Mo, S.; Nicola, P.; Yung-Eun, S. Highly Ordered and Vertically Oriented TiO_2/Al_2O_3 Nanotube Electrodes for Application in Dye-Sensitized Solar Cells. *Nanotechnology* **2014**, *25 (50)*, 504003.

(32) Gui, Q.; Zhen, X.; Zhang, H.; Cheng, C.; Zhu, X.; Yin, M.; Song, Y.; Lu, L.; Chen, X.; Li, D. Enhanced Photoelectrochemical Water Splitting Performance of Anodic TiO_2 Nanotube Arrays by Surface Passivation. *ACS Appl. Mater. Interfaces* **2014**, *6*, 17053-17058.

(33) Zeng, M.; Peng, X.; Liao, J.; Wang, G.; Li, Y.; Li, J.; Qin, Y.; Wilson, J.; Song, A.; Lin, S. Enhanced Photoelectrochemical Performance of Quantum Dot-Sensitized TiO_2 Nanotube Arrays with Al_2O_3 Overcoating by Atomic Layer Deposition. *Phys. Chem. Chem. Phys*. **2016**, *18*, 17404-17413.

(34) Cai, H.; You, Q.; Hu, Z.; Duan, Z.;, Cui, Y.; Sun, J.; Xu, N.; Wu, J. Fabrication and Correlation between Photoluminescenceand Photoelectrochemical Properties of Vertically Aligned ZnO coated TiO_2 Nanotube Arrays. *Solar Energy Materials&Solar Cells* **2014**, *123*, 233–238.

(35) Jeong, J.-S.; Choe, B.-H.; Lee, J.-H.; Lee, J.-J.; Choi, W.-Y. ZnO-Coated TiO_2 Nanotube Arrays for a Photoelectrode in Dye-Sensitized Solar Cells. *J. Electron. Mater.* **2014**, 43, 375-380.

(36) Zazpe, R.; Knaut, M.; Sopha, H.; Hromadko, L.; Albert, M.; Prikryl, J.; Gärtnerová, V.; Bartha, J. W.; Macak, J. M. Atomic Layer Deposition for Coating of High Aspect Ratio TiO_2 Nanotube Layers. *Langmuir* **2016**, *32*, 10551–10558.

(37) Sopha, H.; Hromadko, L.; Nechvilova, K.; Macak, J. M. Effect of Electrolyte Age and Potential Changes on the Morphology of TiO_2 Nanotubes. *Journal of Electroanalytical Chemistry* **2015**, *759*, 122–128.

(38) Macak, J. M.; Prikryl, J.; Sopha, H.; Strizik, L. Antireflection ln_2O_3 Coatings of Self-Organized TiO_2 Nanotube Layers Prepared by Atomic Layer Deposition. *Phys. Status Solidi RRL* **2015**, *9*, 516-520.

(39) Acevedo-Peña, P.; Carrera-Crespo, J. E.; Gonzalez, F.; Gonzalez, I. Effect of Heat Treatment on the Crystal Phase Composition, Semiconducting Properties and Photoelectrocatalytic Color Removal Efficiency of TiO_2 Nanotubes Arrays. *Electrochimica Acta* **2010**, *140*, 564-571.

(40) Hanaor, D. A. H.; Sorrell, C. C. Review of the Anatase to the Rutile Phase Transformation. *J. Mater. Sci*. **2011**, *46*, 855-874.

(41) Lu, J.; Fu, B.; Kung, M. C.; Xiao, G.; Elam, J. W.; Kung, H. H.; Stair, P. C. Coking-and Sintering-Resistant Palladium Catalyst Achieved Through Atomic Layer Deposition. *Science* **2012**, *335*, 1205-1208.

(42) Ma, L.; Huang, Y.; Hou, M.; Xie, Z.; Zhang, Z. Silver Nanorods Wrapped with Ultrathin Al_2O_3 Layers Exhibiting Excellent SERS Sensitivity and Outstanding SERS Stability. *Scientific Reports* **2015**, *5*, 12890.

(43) Rath, C.; Mohanty, P.; Pandey, A. C.; Mishra, N. C. Oxygen Vacancy Induced Structural Phase Transformation in TiO_2 Nanoparticles. *J. Phys. D: Appl. Phys.* **2009**, *42*, 205101.

(44) Reidy, D. J.; Holmes, J. D.; Morris, M. A. The Critical Size Mechanism for the Anatase to Rutile Transformation in TiO_2 and Doped-TiO_2. *J. Eur. Ceram.Soc*. **2006**, *6*, 1527-1534.

(45) Zhang, Y. H.; Xiao, P.; Zhou, X.Y.; Liu, D.W.; Garcia, B.B.; Cao, G.Z. Carbon Monoxide Annealed TiO_2 Nanotube Array Electrodes for Efficient Biosensor Applications. *J. Mater. Chem.* **2009**, *19*, 948–953.

(46) Varghese, O. K.; Gong, D.; Paulose, M.; Grimes, C. A.; Dickey, E. C. Crystallization and High-Temperature Structural Stability of Titanium Oxide Nanotube Arrays. *J. Mater. Res.* **2003**, *18*, 156-165.

(47) Zhu, K.; Neale, N. R.; Halverson, A. F.; Kim, J. Y.; Frank, A. J. Effects of Annealing Temperature on the Charge-Collection and Light-Harvesting Properties of TiO_2 Nanotube-Based Dye-Sensitized Solar Cells. *J. Phys. Chem. C* **2010**, *114*, 13433-13441.

(48) Yu, J.; Wang, B. Effect of Calcination Temperature on Morphology and Photoelectrochemical Properties of Anodized Titanium Dioxide Nanotube Arrays. *Appl. Catal. B-Environ.* **2010**, *94*, 295-302.

(49) So, S.; Hwang, I.; Riboni, F.; Yoo, J.; Schmuki, P. Robust Free Standing Flow-Through TiO_2 Nanotube Membranes of Pure Anatase. *Electrochemistry Comm.* **2016**, *71*, 73-78.

(50) Baggetto, L.; Charvillat, C.; Thebault, Y.; Esvan. J.; Lafont, M.-C.; Scheid, E.; Veith, G. M.; Vahlas, C. Amorphous Alumina Thin Films Deposited on Titanium: Interfacial Chemistry and Thermal Oxidation Barrier Properties. *Phys. Status Solidi A* **2016**, *213*, 470-480.

(51) Albu, S. P.; Ghicov, A.; Macak, J. M.; Hahn, R.; Schmuki. P. Self-Organized, Free-Standing TiO_2 Nanotube Membrane for Flow-through Photocatalytic Applications. *Nano Lett.* **2007**, *7*, 1286–1289.

(52) Crawford, G.A.; Chawla, N.; Das, K.; Bose, S.; Bandyopadhyay, A. Microstructure and Deformation Behavior of Biocompatible TiO_2 Nanotubes on Titanium Substrate. *Acta Biomaterialia* **2007**, *3*, 359–367.

(53) Crawford, G. A.; Chawla, N.; Houston, J. E. Nanomechanics of Biocompatible TiO_2 Nanotubes by Interfacial Force Microscopy (IFM). *J. Mech. Behav. Biomed. Mater*. **2009**, *2*, 580-587.

(54) Schmidt-Stein, F.; Thiemann, S.; Berger, S.; Hahn, R.; Schmuki, P. Mechanical Properties of Anatase and Semi-Metallic TiO_2 Nanotubes. *Acta Materialia* **2010**, *58*, 6317–6323.

(55) Hirakata, H.; Ito, H.; Yonezu, A.; Tsuchiya, H.; Fujimoto, S.; Minoshima, K. Strength of Self-Organized TiO_2 Nanotube Arrays. *Acta Materiala* **2010**, *5*, 4956-4967.

(56) Chang, W.-Y.; Fang, T.-H.; Chiu, Z.-W.; Hsiao, Y.-J.; Ji, L.-W. Nanomechanical Properties of Array TiO_2 Nanotubes. *Micropor. Mesopor. Mat*. **2011**, *145*, 87-92.

(57) Zalnezhad, E.; Hamouda, A. M. S.; Faraji, G.; Shamshirband, S. TiO_2 Nanotube Coating on Stainless Steel 304 for Biomedical Applications. *Ceramic International* **2015**, *41*, 2785-2793.

(58) Xu, Y. N.; Liu, M.N.; Wang, M. C.; Oloyede, A.; Bell, J. M.; Yan, C. Nanoindentation Study of the Mechanical Behavior of TiO_2 Nanotube Arrays. *J. Appl. Phys*. **2015**, *118*, 145301.

(59) Munirathinam, B.; Neelakantan, L. Role of Crystallinity on the Nanomechanical and Electrochemical Properties of TiO_2 Nanotubes. *J. Electroanal. Chem*. **2016**, *770*, 73-83.

(60) Correa, G. C.; Bao, B.; Strandwitz, N. C. Chemical Stability of Titania and Alumina Thin Films Formed by Atomic Layer Deposition. *ACS Appl. Mater. Interfaces* **2015,** *7 (27)***,** 14816–14821.

(61) Lefèvre, G.; Duc, M.; Lepeut, P.; Caplain, R.; Fédoroff, M. Hydration of γ-Alumina in Water and Its Effects on Surface Reactivity. *Langmuir* **2002**, *18 (20)*, 7530–7537.

(62) Ganapathy, V.; Karunagaran, B.; Rhee, S. W. Improved Performance of Dye-Sensitized Solar Cells with TiO_2/Alumina Core–Shell Formation Using Atomic Layer Deposition. *J. Power Sources* **2010**, *195*, 5138-5143.

Table of contents

High-aspect ratio anodic TiO_2 nanotube layers were coated by additional Al_2O_3 layers using atomic layer deposition, resulting in very remarkable enhanced thermal, chemical and mechanical stability. This enables to spread the application of anodic TiO_2 nanotube layers to higher temperatures than before (870°C) and extremely acidic conditions, not feasible before.